

## Supporting Information

# Molecular Cocrystals with Hydrogen-Bonded Polymeric Structures and Polarized Luminescence

Jing-Yi Zhao <sup>1,2</sup>, Fa-Feng Xu <sup>1,\*</sup>, Zhong-Qiu Li <sup>1</sup>, Zhong-Liang Gong <sup>1</sup>, Yu-Wu Zhong <sup>1,2,\*</sup>, and Jiannian Yao <sup>1,2,\*</sup>

<sup>1</sup>Beijing National Laboratory for Molecular Sciences, CAS Key Laboratory of Photochemistry, CAS Research/Education Center for Excellence in Molecular Sciences, Institute of Chemistry, Chinese Academy of Sciences, Beijing 100190, China

<sup>2</sup>School of Chemical Sciences, University of Chinese Academy of Sciences, Beijing 100049, China

\*E-mail: xufafeng@iccas.ac.cn; zhongyuwu@iccas.ac.cn; jnyao@iccas.ac.cn

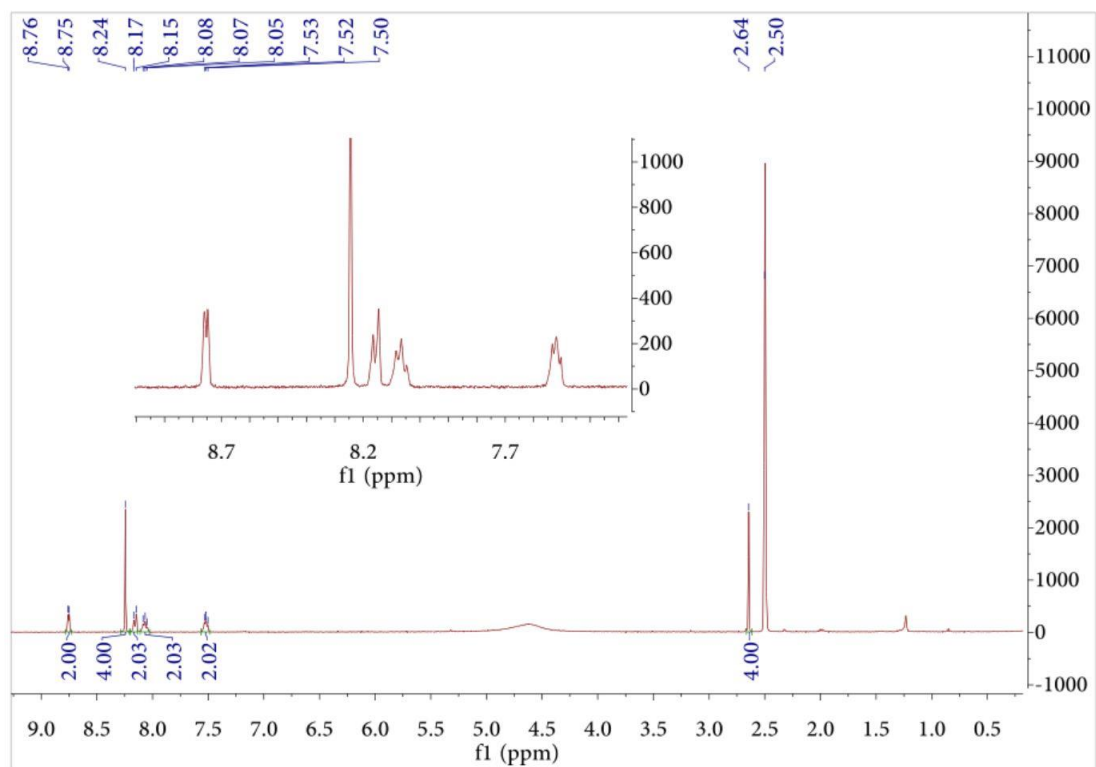


**Figure S1.**  $^1\text{H}$  NMR spectrum of **4** in  $\text{DMSO-d}_6$ .

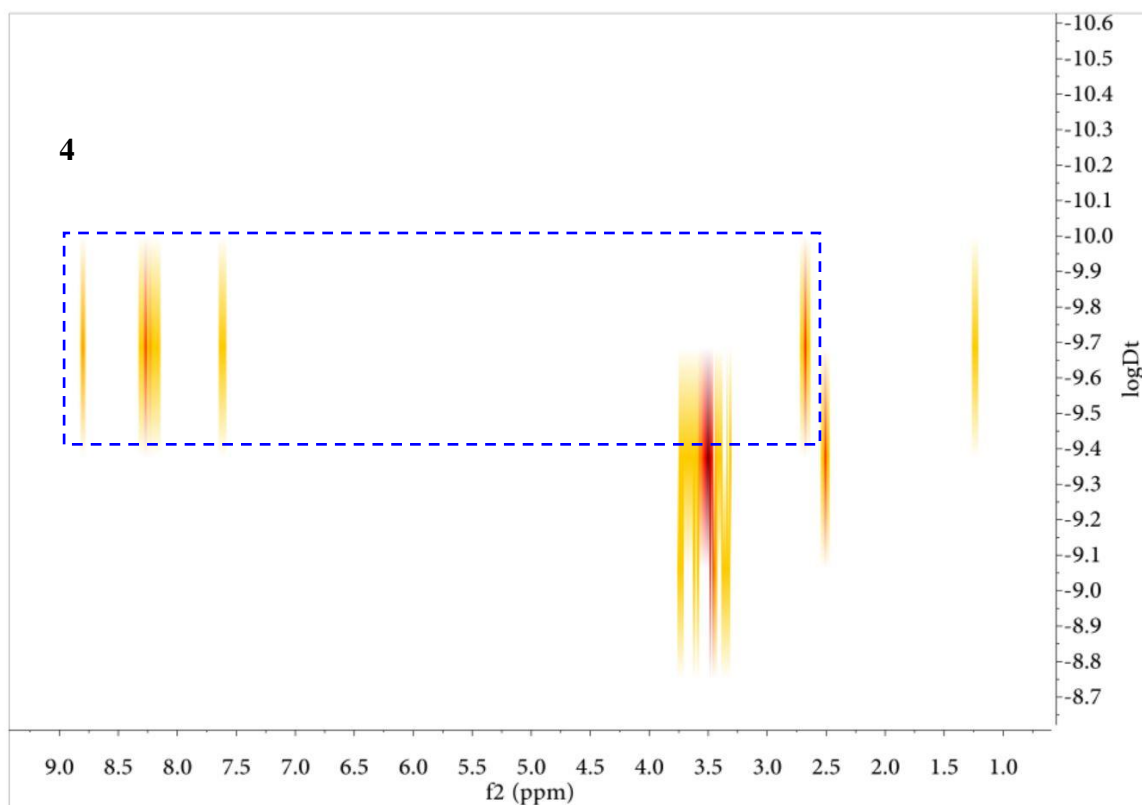


**Figure S2.**  $^1\text{H}$  DOSY NMR spectrum of **4** in  $\text{DMSO-d}_6$ .

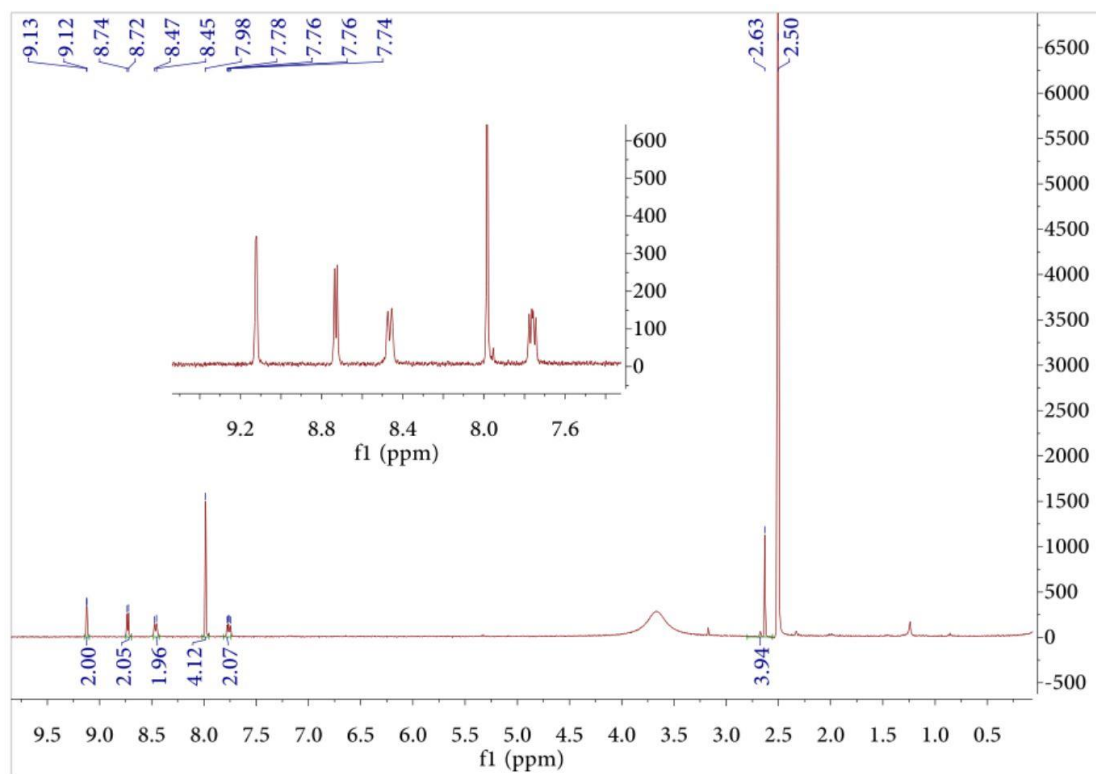


**Figure S3.**  $^1\text{H}$  NMR spectrum of **5** in  $\text{DMSO-d}_6$ .

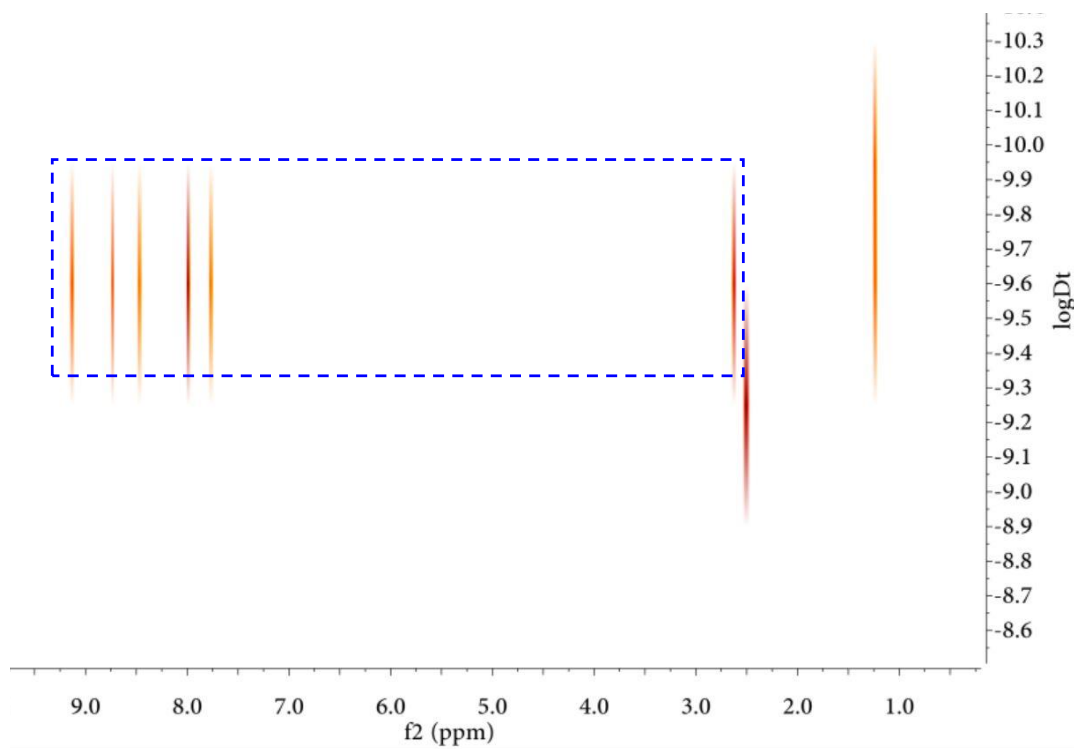


**Figure S4.**  $^1\text{H}$  DOSY NMR spectrum of **5** in  $\text{DMSO-d}_6$ .

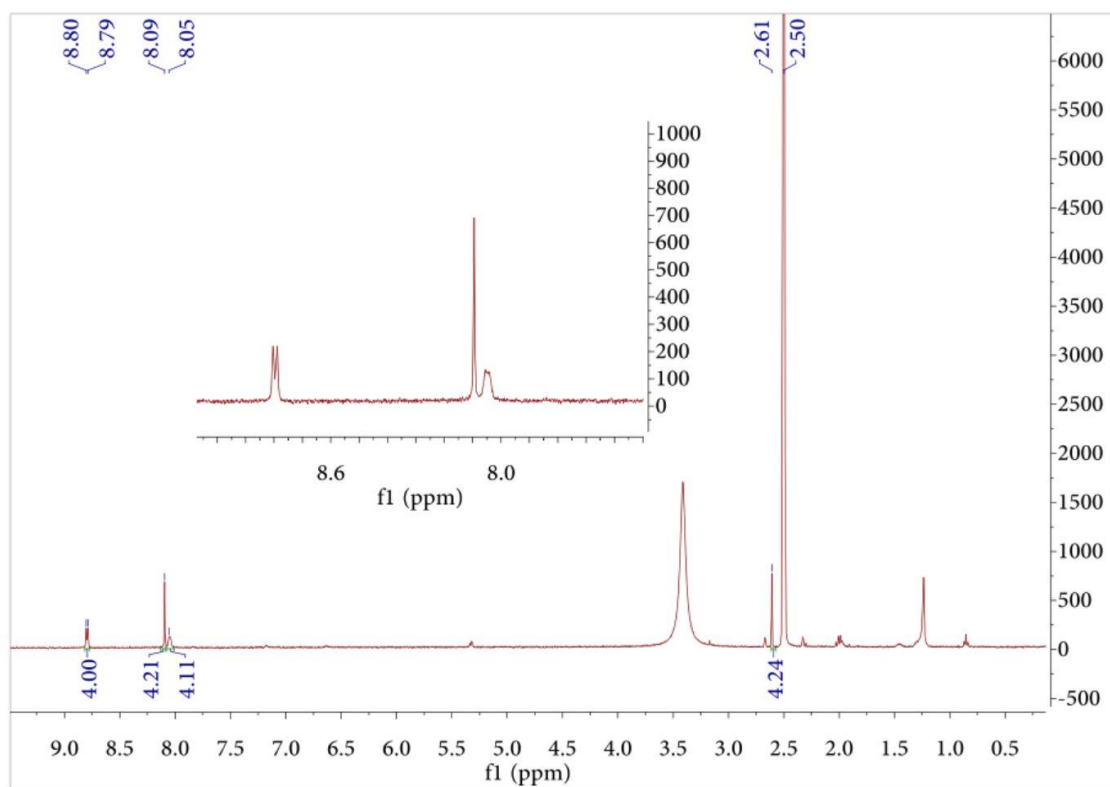


**Figure S5.**  $^1\text{H}$  NMR spectrum of **6** in  $\text{DMSO-d}_6$ .

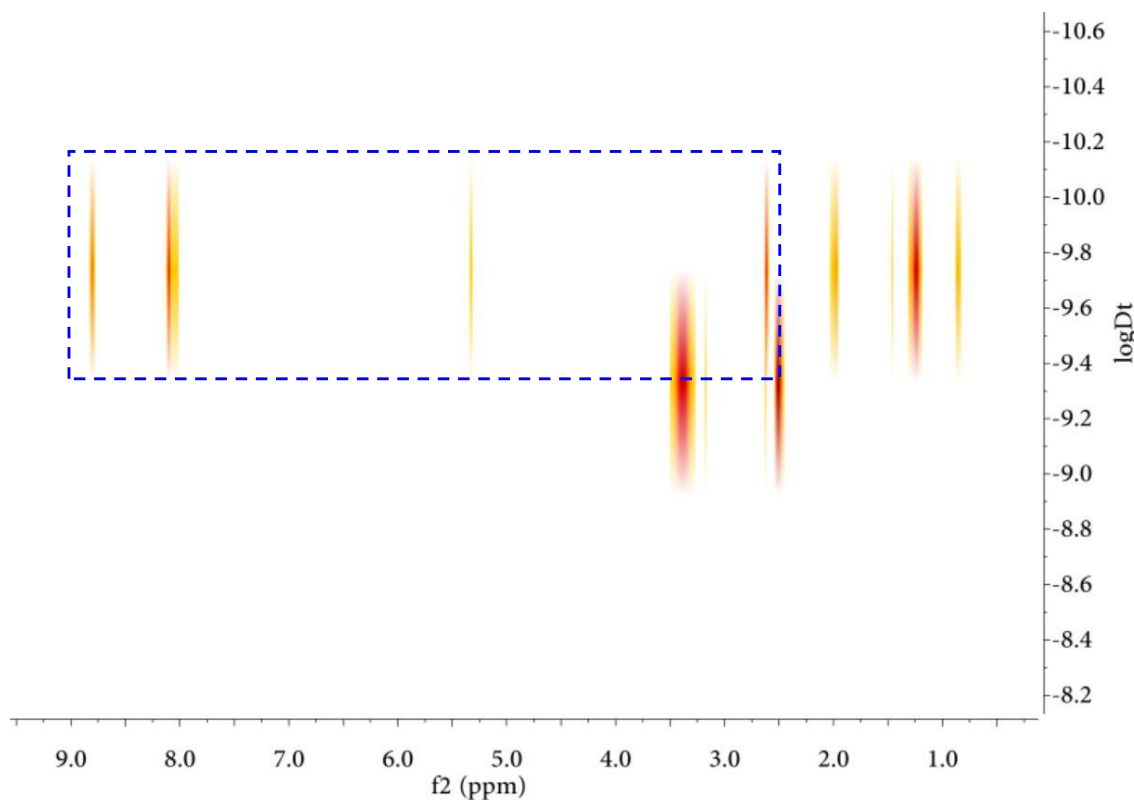


**Figure S6.**  $^1\text{H}$  DOSY NMR spectrum of **6** in  $\text{DMSO-d}_6$ .

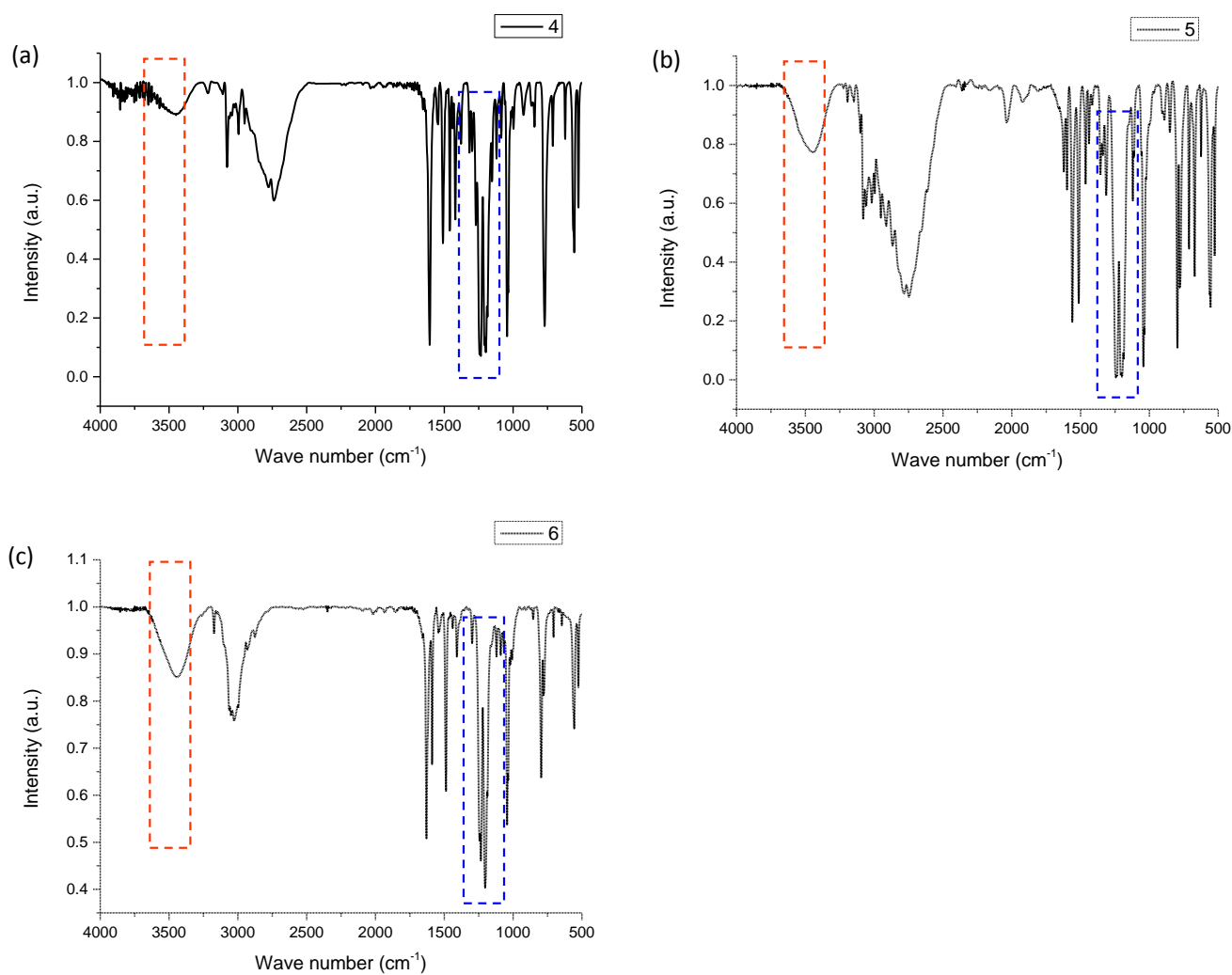


**Figure S7.** FTIR spectrum of the microcrystals of (a) **4**, (b) **5**, and (c) **6** as KBr pellet. The bands at around 3500 cm<sup>-1</sup> are assigned to the vibrations of hydrogen bonds. The two bands at around 1200 cm<sup>-1</sup> are ascribed to the symmetric and asymmetric stretching vibrations of the sulfonate groups.

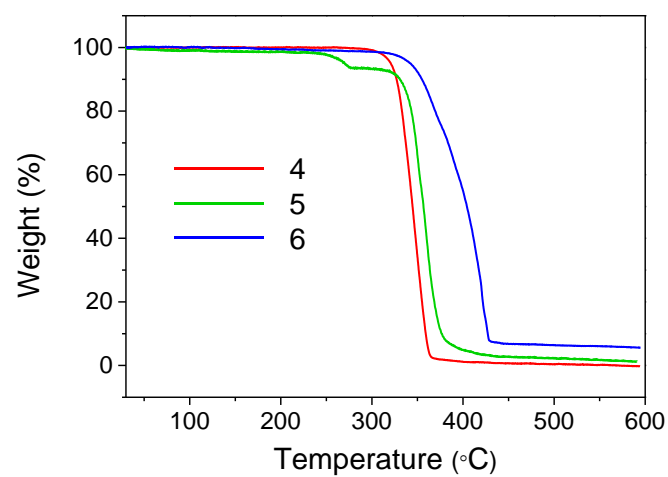


**Figure S8.** Thermogravimetric analysis (TGA) of the microcrystals of **4**, **5**, and **6** with a temperature rate of 10 °C /min in a nitrogen environment (200 mL/min).

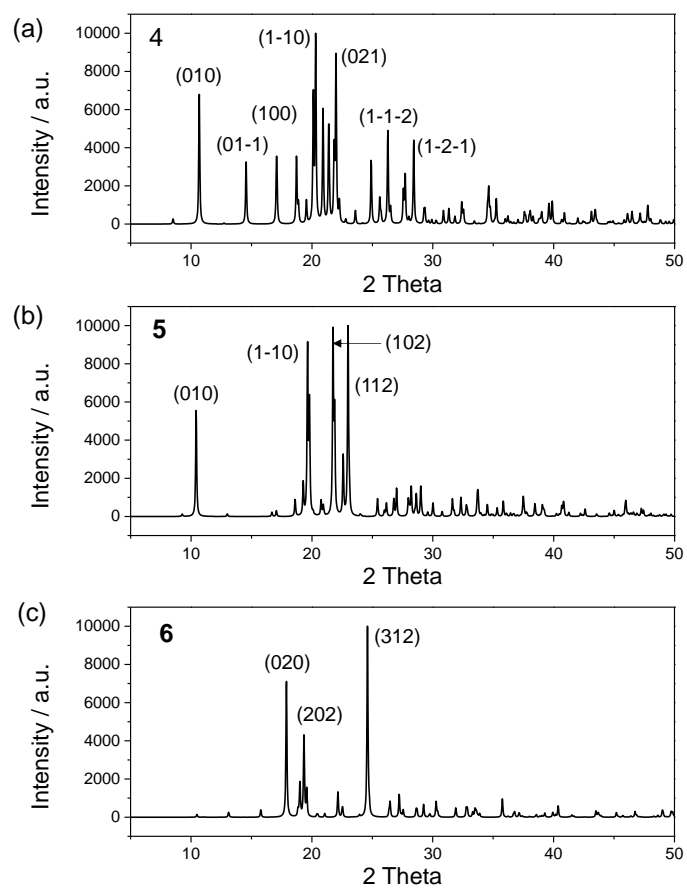


**Figure S9.** Simulated powder XRD patterns of (a) **4**, (b) **5**, and (c) **6** based on their single-crystal data.

**Table S1.** Photophysics data of microcrystals of **4** – **6**.<sup>a</sup>

Compound	$\lambda_{\text{emi}}/\text{nm}$	$\Phi/\%$	$\tau/\text{ns}$	$k_r/10^7 \text{ s}^{-1}$	$k_{\text{nr}}/10^7 \text{ s}^{-1}$
<b>4</b>	385	12.9	4.8	2.67	18.03
<b>5</b>	456	27.7	11.7	2.38	6.20
<b>6</b>	466	18.0	1.8	9.94	45.30

<sup>a</sup> $\Phi$  is absolute quantum yield.  $\tau$  is averaged life time. See further details in Figure S2.  $k_r = \Phi/\tau$ ;  $k_{\text{nr}} = (1 - \Phi)/\tau$ .

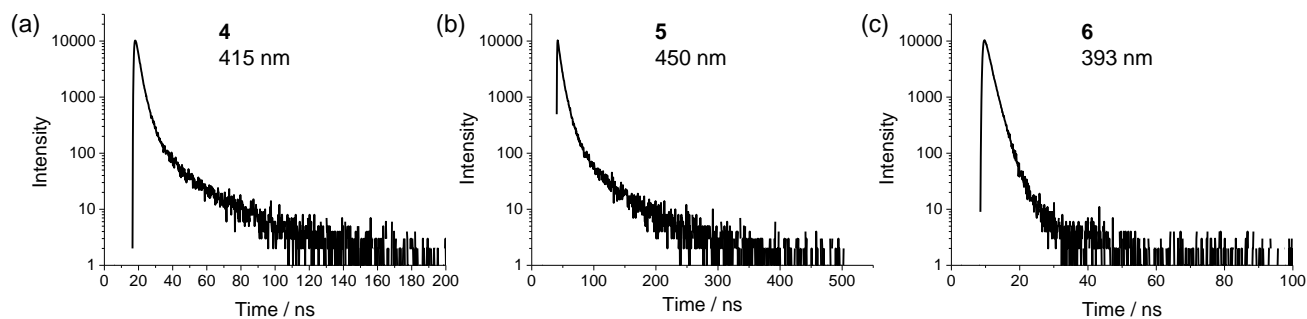


**Figure S10.** Lifetime decay curves for microcrystals of (a) **4**, (b) **5**, and (c) **6**.

Decay curves for microcrystals of **4**, and **5** are tri-exponentially fitted and the decay of **6** is bi-exponentially fitted. The average lifetimes ( $\tau_{\text{ave}}$ ) are reported in Table S1, which are determined by  $\tau_{\text{ave}} = \alpha_1\tau_1 + \alpha_2\tau_2 + \alpha_3\tau_3$ .

For microcrystals of **4**,  $\tau_{\text{ave}} = 4.83 \text{ ns}$ ,  $\tau_1 = 2.27 \text{ ns}$ ,  $\tau_2 = 6.56 \text{ ns}$ ,  $\tau_3 = 24.11 \text{ ns}$ ,  $\alpha_1 = 74.9\%$ ,  $\alpha_2 = 16.7\%$ ,  $\alpha_3 = 8.4\%$ ;

for microcrystals of **5**,  $\tau_{\text{ave}} = 11.66 \text{ ns}$ ,  $\tau_1 = 3.72 \text{ ns}$ ,  $\tau_2 = 8.70 \text{ ns}$ ,  $\tau_3 = 42.34 \text{ ns}$ ,  $\alpha_1 = 32.0\%$ ,  $\alpha_2 = 54.4\%$ ,  $\alpha_3 = 13.6\%$ ;

for microcrystals of **6**,  $\tau_{\text{ave}} = 1.81 \text{ ns}$ ,  $\tau_1 = 1.53 \text{ ns}$ ,  $\tau_2 = 3.47 \text{ ns}$ ,  $\alpha_1 = 85.8\%$ ,  $\alpha_2 = 14.2\%$ .

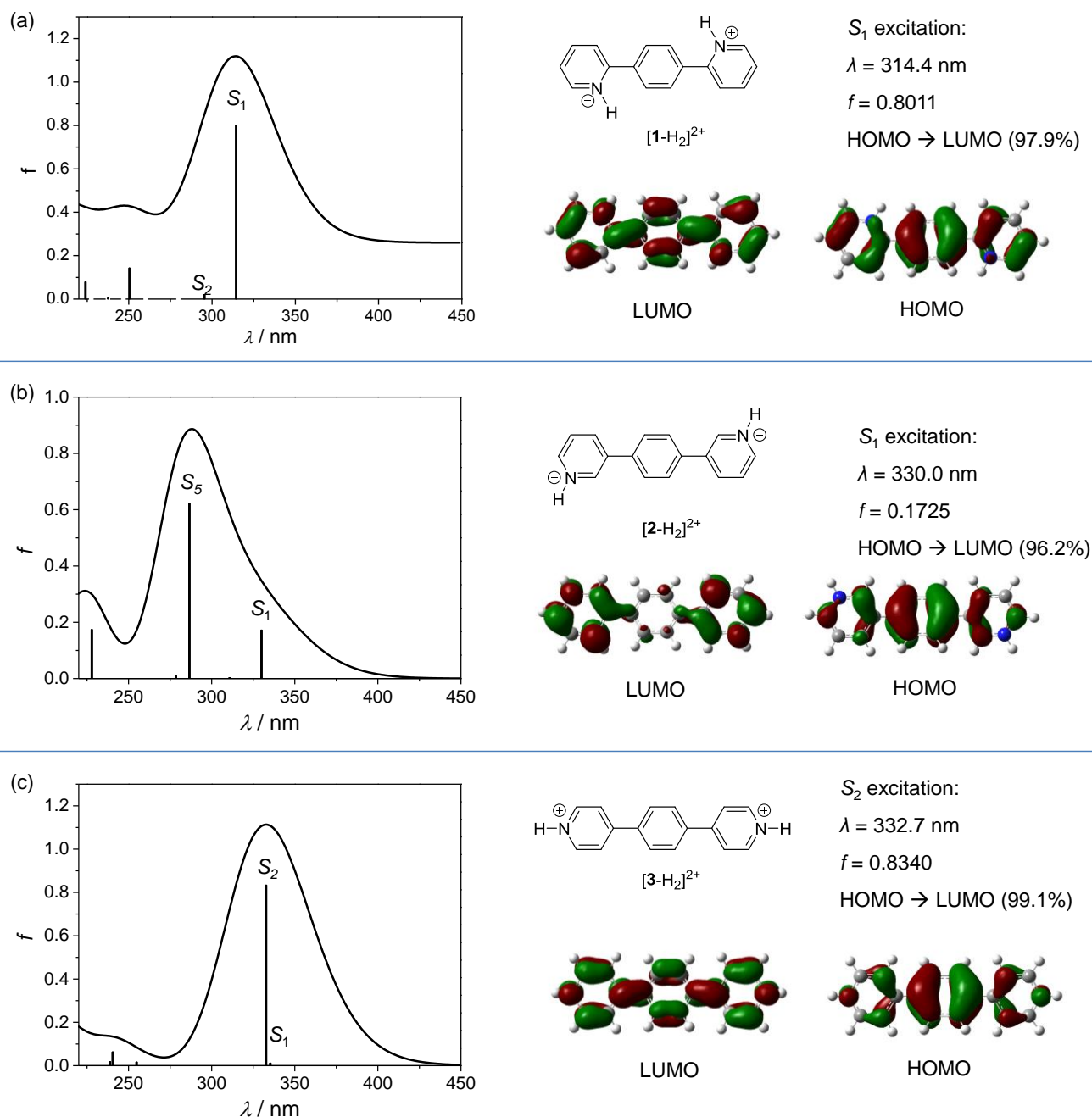


**Figure S11.** TDDFT calculation results of (a)  $[1-H_2]^{2+}$ , (b)  $[2-H_2]^{2+}$ , and (c)  $[3-H_2]^{2+}$ . Left: TDDFT-predicted vertical excitations. Right: chemical structures, DFT-calculated frontier orbitals, and the calculated wavelength ( $\lambda$ ), oscillator strength ( $f$ ), and percent contribution for the HOMO $\rightarrow$ LUMO excitation.

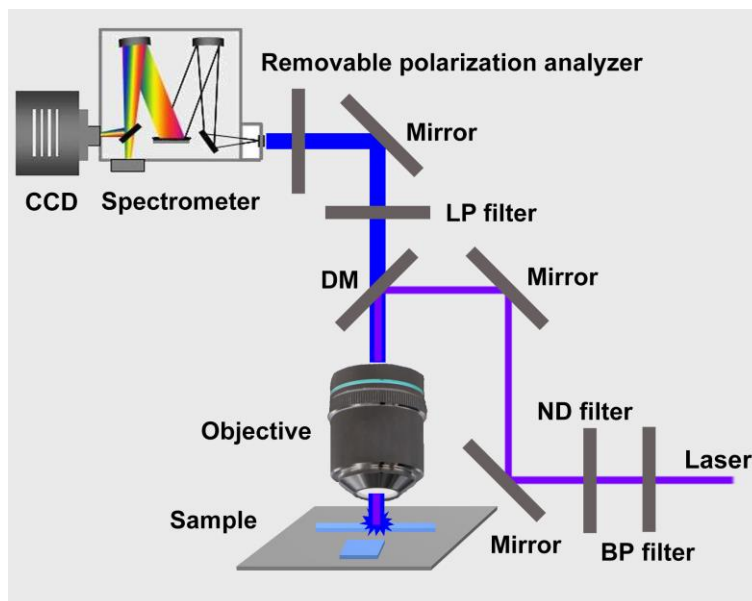


**Figure S12.** Schematic demonstration of the experimental setup for polarized luminescence characterization for a single microcrystal. CCD: charge coupled device; LP filter: long-pass filter; DM: dichroic mirror; ND filter: neutral density filter; BP filter: band-pass filter. The polarization luminescence information of the microcrystal is probed by a removable polarization analyzer plate.

The excitation laser beam (CW, 405 nm) was filtered with a 405/10 nm band-pass filter and then focused down to a 10- $\mu\text{m}$  diameter spot through an objective lens (Olympus M Plan,  $\times 20$ , N.A. = 0.4) as a nearly uniform pump source. The power at the input was altered by a neutral density filter. The emissions from individual microcrystals were collected by the same objective with a back-scattering configuration and analyzed by Princeton Instrument HRS-300S spectrometer with a thermoelectric-cooled PIXIS 256BR CCD after removing the excitation beam with a 420-nm long-pass filter. The removable polarization analyzer was used before the spectrometer when collecting polarized luminescent spectra of the microcrystals.